Identification of a New Reaction Intermediate in the Oxidation of Methylamine Dehydrogenase by Amicyanin†

Zhenyu Zhu and Victor L. Davidson*

Department of Biochemistry, The University of Mississippi Medical Center, Jackson, Mississippi 39216-4505

Received December 15, 1998; Revised Manuscript Received February 17, 1999

ABSTRACT: The two-electron oxidation of tryptophan tryptophylquinone (TTQ) in substrate-reduced methylamine dehydrogenase (MADH) by amicyanin is known to proceed via an *N*-semiquinone intermediate in which the substrate-derived amino group remains covalently attached to TTQ [Bishop, G. R., and Davidson, V. L. (1996) *Biochemistry 35*, 8948−8954]. A new method for the stoichiometric formation of the *N*-semiquinone in vitro has allowed the study of the oxidation of the *N*-semiquinone by amicyanin in greater detail than was previously possible. Conversion of *N*-semiquinone TTQ to the quinone requires two biochemical events, electron transfer to amicyanin and release of ammonia from TTQ. Using rapid-scanning stopped-flow spectroscopy, it is shown that this occurs by a sequential mechanism in which oxidation to an imine (*N*-quinone) precedes hydrolysis by water and ammonia release. Under certain reaction conditions, the *N*-quinone intermediate accumulates prior to the relatively slow hydrolysis step. Correlation of these transient kinetic data with steady-state kinetic data indicates that the slow hydrolysis of the *N*-quinone by water does not occur in the steady state. In the presence of excess substrate, the next methylamine molecule initiates a nucleophilic attack of the *N*-quinone TTQ, causing release of ammonia that is concomitant with the formation of the next enzyme−substrate cofactor adduct. In light of these results, the usually accepted steady-state reaction mechanism of MADH is revised and clarified to indicate that reactions of the quinone form of TTQ are side reactions of the normal catalytic pathway. The relevance of these conclusions to the reaction mechanisms of other enzymes with carbonyl cofactors, the reactions of which proceed via Schiff base intermediates, is also discussed.

Methylamine dehydrogenase (MADH)[1] (*1*) catalyzes the oxidative deamination of methylamine and mediates electron transfer from methylamine to a type I blue copper protein, amicyanin (Ami in eq 1) (*2*).

$$CH_3NH_2 + H_2O + 2\text{Ami}(Cu^{2+}) \rightarrow NH_3 + HCHO + 2\text{Ami}(Cu^{+}) + 2H^{+} \quad (1)$$

The substrate-derived electrons are then transferred to one or more *c*-type cytochromes (*3*), and then to O_2 via cytochrome oxidase. MADH uses the tryptophan tryptophylquinone (TTQ, Figure 1) prosthetic group (*4*) which is posttranslationally formed from two tryptophan residues. As the reduction of TTQ is a two-electron transfer step, and the oxidation of MADH occurs via two one-electron transfer steps, the overall reaction can be separated into the following partial reactions (eqs 2−4). The different redox forms of TTQ in Eqs 2−4 are shown in Figure 1.

$$CH_3NH_2 + O\text{-quinone} \rightarrow HCHO + N\text{-quinol} + H^{+} \quad (2)$$

$$N\text{-quinol} + \text{Ami}(Cu^{2+}) \rightarrow N\text{-semiquinone} + \text{Ami}(Cu^{+}) + H^{+} \quad (3)$$

$$N\text{-semiquinone} + \text{Ami}(Cu^{2+}) + H_2O \rightarrow O\text{-quinone} + \text{Ami}(Cu^{+}) + NH_3 \quad (4)$$

The existence of the *N*-semiquinone reaction intermediate has been proven by kinetic methods (*5*) and ENDOR and ESEEM spectroscopy (*6*). Potentiometric studies demonstrated that the O at C7 is unprotonated in the quinol and semiquinone forms of TTQ (*7*). This unusual feature provides stabilization of the *N*-quinol and *N*-semiquinone reaction intermediates.

The partial reaction shown in eq 4 includes two biochemical events, oxidation of *N*-semiquinone TTQ by amicyanin and release of ammonia from TTQ. This could occur either by a concerted mechanism in which electron transfer is concomitant with ammonia release or by a sequential mechanism in which oxidation to an imine (*N*-quinone in Figure 1) precedes hydrolysis and ammonia release. It was previously possible to characterize in detail the partial reaction in eq 3 (*8*, *9*) because it was possible to generate a stable *N*-quinol with which to initiate the reaction with

† This work was supported by National Institutes of Health Grant GM-41574.

* Corresponding author: Department of Biochemistry, The University of Mississippi Medical Center, 2500 N. State St., Jackson, MS 39216-4505. Telephone: (601) 984-1515. Fax: (601) 984-1501. E-mail: vdavidson@biochem.umsmed.edu.

[1] Abbreviations: MADH, methylamine dehydrogenase; TTQ, tryptophan tryptophylquinone; BTP, BisTris propane [1,3-bis[tris(hydroxymethylamino)]propane]; *O*-quinol, fully reduced TTQ with oxygen at C6; *O*-semiquinone, semiquinone TTQ with oxygen at C6; *N*-quinol, fully reduced TTQ with nitrogen bonded to C6; *N*-semiquinone, semiquinone TTQ with nitrogen bonded to C6; KSIE, kinetic solvent isotope effect; PLP, pyridoxal phosphate.

10.1021/bi982939r CCC: $18.00
Published on Web 03/24/1999

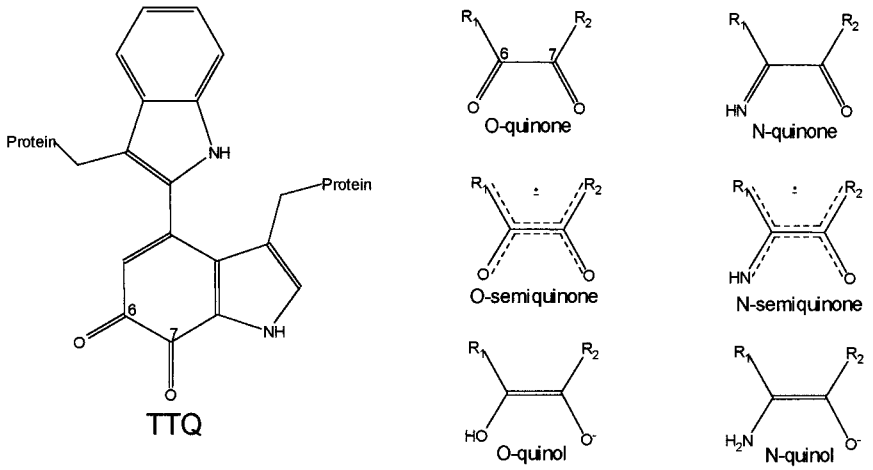

FIGURE 1: Structure of TTQ and its derivatives. Carbonyl C6 and C7 are labeled in the *O*-quinone structures. R_1 and R_2 indicate connections to the remainder of the TTQ ring in the structures of the different redox forms.

amicyanin. Analysis of the oxidation of the *N*-semiquinone (eq 4), however, has been hampered by the inability to generate the pure *N*-semiquinone in vitro. It was possible to study the oxidation of the *N*-semiquinone under certain reaction conditions by analyzing the complete oxidation of the *N*-quinol by excess amicyanin. Rate constants for both one-electron transfer steps could be extracted from a two-exponential fit of kinetic data for the overall reaction (*5*). If eq 4 were a two-step sequential process, it would be very difficult to distinguish it from a one-step concerted process by this method as that would require a three-exponential fit of the overall reaction that was capable of discerning rapid and subtle spectral changes. Given the typical levels of noise in such experiments, one could not reasonably distinguish between a two- or three-exponential fit of these data. The previous method for forming the *N*-semiquinone in vitro was by comproportionation of *O*-quinone MADH and *N*-quinol MADH at alkaline pH (*10*). The result is a mixture which contains both *N*-semiquinone and *O*-semiquinone, as well as some fully oxidized and reduced MADH. This sample was used to initiate the reaction with amicyanin and verify the rate constants for the oxidation of *N*-semiquinone which were obtained from the two-exponential fits of the complete oxidation of *N*-quinol MADH by excess amicyanin (*11*). However, with this poorly defined mixture, it was not possible to address the question of whether any kinetically distinguishable intermediate was formed during the partial reaction depicted in eq 4.

We recently reported that *N*-quinol MADH was converted to a semiquinone form when exposed to long-wavelength UV light in the presence of O_2 (*12*). This has allowed us to develop a method by which to generate an essentially pure *N*-semiquinone sample with which we can study the partial reaction depicted in eq 4. Results are presented that prove that the oxidation of the *N*-semiquinone by amicyanin occurs by a sequential mechanism that proceeds via an iminoquinone (*N*-quinone) intermediate. The kinetic and spectroscopic properties of this intermediate are characterized, as well as its role in the overall steady-state reaction of MADH with methylamine and amicyanin. These results indicate that the substrate amine reacts with the *N*-quinone in the steady state, and that its hydrolysis to the *O*-quinone need not occur. On the basis of these results, a revised catalytic mechanism for the overall reaction of MADH with methylamine and amicyanin is presented and the relevance of these findings to the reaction mechanisms of other carbonyl cofactors such as topaquinone and pyridoxal phosphate is discussed.

EXPERIMENTAL PROCEDURES

Purification of MADH (*13*) and amicyanin (*2*) from *Paracoccus denitrificans* (ATCC 13543) was carried out as described previously. Protein concentrations were determined from the previously reported extinction coefficients of MADH (*14*) and amicyanin (*2*). All experiments were performed in 10 mM BisTris propane (BTP) buffer, at the indicated pH. All reagents were obtained from commercial sources.

N-Semiquinone MADH was prepared by exposing *N*-quinol MADH to long-wavelength UV light (*12*). MADH was first reduced by stoichiometric addition of methylamine. The sample was then placed in a quartz cuvette and irradiated with a Rad-Free RF UV-365 Long-Wave UV Lamp (Schleicher & Schleicher) placed approximately 3 in. from the sample. The formation of the *N*-semiquinone was monitored spectrophotometrically (*12*) and was typically complete after about 5 min with a yield of approximately 95%.

O-Semiquinone MADH was prepared by two methods. As described previously (*14*), it was prepared by anaerobic titration with one electron equivalent per TTQ of dithionite. It was also prepared as described above by controlled irradiation of dithionite-generated *O*-quinol MADH with long-wavelength UV light.

Steady-state kinetic experiments were performed as described previously (*15*). The assay mixture contained 20 nM MADH, 100 μM methylamine, and 100 μM amicyanin. The reaction was initiated by the addition of methylamine, and activity was monitored by the change in absorbance at 595 nm caused by the reduction of amicyanin. Assays were performed at 25 °C. Data were fit to eq 5.

$$v/[E] = k_{cat}[S]/(K_m + [S]) \quad (5)$$

An On-Line Instrument Systems (OLIS) RSM 1000 rapid-scanning stopped-flow spectrophotometer was used for transient kinetic experiments. Unless otherwise indicated, reactions were initiated by mixing 4 μM MADH with 40 μM amicyanin at 25 °C under the indicated buffer conditions. This concentration of amicyanin was sufficient to maintain

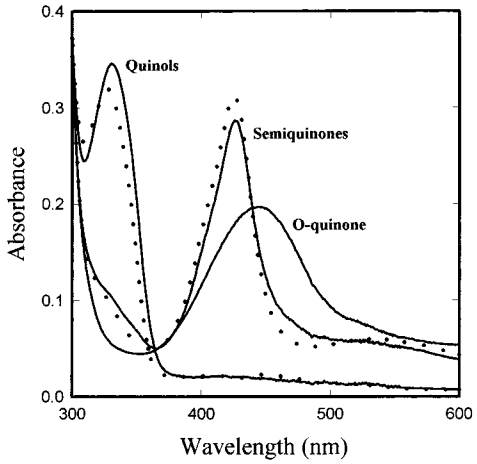

FIGURE 2: Absorption spectra of different redox forms of MADH. All spectra were recorded in 6.7 μM MADH in 10 mM BTP buffer at pH 7.5 and 25 °C. Spectra of the *O*-quinone, *O*-semiquinone, and *O*-quinol are displayed as solid lines. Spectra of the *N*-semiquinone and *N*-quinol are displayed as dotted lines.

pseudo-first-order reaction conditions and saturate the reaction. Raising the amicyanin concentration to 200 μM yielded identical results. Data were fitted either by global kinetic and factor analysis using the OLIS software, as described previously (*5*), or by analysis of the change in absorbance with time at selected single wavelengths as indicated.

RESULTS AND DISCUSSION

Absorption Spectrum of N-Semiquinone MADH. Since it had not previously been possible to generate a pure sample of the *N*-semiquinone in vitro, it was not possible to exactly determine its absorption spectrum. In previous kinetic studies (*5*), it was possible to reconstruct the putative spectrum of the *N*-semiquinone intermediate from the global and factor analysis of the biphasic spectral changes associated with the complete oxidation of *N*-quinol MADH by amicyanin. Spectral reconstruction suggested that the *N*-semiquinone exhibited an absorption maximum identical to that of the *O*-semiquinone, which can be generated in a pure form in vitro (*14*). The extinction coefficient for the main peak, however, appeared to be significantly smaller than that of the *O*-semiquinone (*5*). Since only fractional accumulation of the *N*-semiquinone occurred, it was not clear whether that decreased extinction coefficient was real or an artifact of the spectral reconstruction analysis. The spectrum of the *N*-semiquinone generated by the new light-dependent method is, in fact, very similar to that of the *O*-semiquinone (Figure 2). The fact that the sample generated by the new method is truly *N*-semiquinone has been verified by EPR spectroscopy (unpublished results). Thus, while the presence of the substrate-derived N on TTQ in semiquinone MADH affects its EPR spectrum (*6*), and reactivity and redox potential (*11*), it has very minor effects on its UV−visible absorption spectrum.

Evidence for an Intermediate in the Oxidation of N-Semiquinone MADH by Amicyanin. The oxidation of *N*-semiquinone MADH by amicyanin (eq 4) was studied in 10 mM BTP at pH values from 7.0 to 9.0. In each case, the reaction was clearly biphasic and a spectral intermediate was observed during the rapid-scanning analysis of the reaction. The results of a representative reaction are shown in Figure

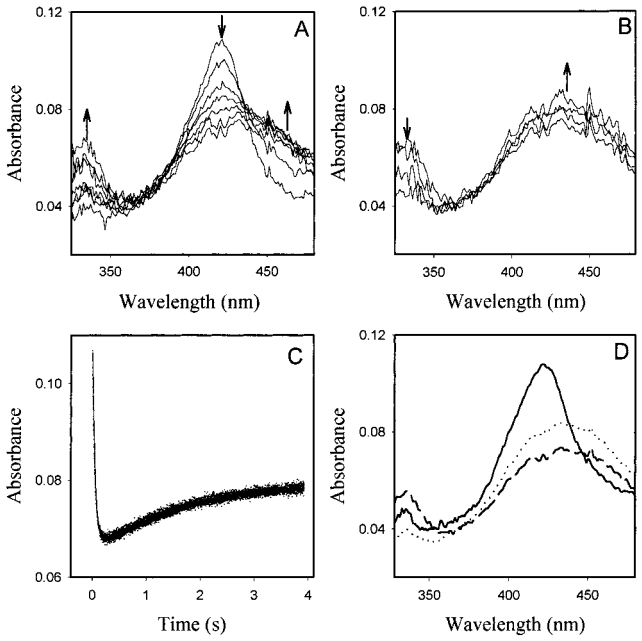

FIGURE 3: Reaction of *N*-semiquinone MADH with amicyanin. The final reaction mixture contained 2 μM MADH and 20 μM amicyanin in 10 mM BTP at pH 7.0 and 25 °C. (A) The first phase of the reaction. Spectra were recorded every millisecond. Those which are displayed were recorded after 1, 17, 33, 49, 65, 81, 129, and 641 ms. Arrows indicate the directions of the spectral changes. (B) The second phase of the reaction. Spectra were recorded every millisecond. Those which are displayed were recorded after 641, 1361, 1601, and 2241 ms. Arrows indicate the directions of the spectral changes. (C) Analysis of the absorbance change with time at 420 nm. The solid line is a fit of the data to eq 6. (D) Calculated spectra. This plot displays a reconstruction of the initial (solid line), intermediate (dashed line), and final (dotted line) absorbing species for the A → B → C mechanism which best describes the data.

3. Inspection of the raw data (Figure 3A,B) reveals that an intermediate species is formed with a spectrum similar to that of the final *O*-quinone product, but with a decreased extinction coefficient for the major peak and an absorption maximum that is slightly shifted relative to that of the quinone. In the wavelength range of 410−460 nm, the major absorption peak falls and then rises. A small increase in absorbance followed by a decrease is also observed at approximately 330 nm. The biphasic nature of the reaction is also clearly seen by monitoring the absorbance at 420 nm with time where a rapid decrease in absorbance is followed by a slow increase (Figure 3C). A single-step reaction mechanism would not exhibit such a complex kinetic pattern. These kinetic data are best fit to a two-exponential equation (eq 6)

$$Y = A_1 e^{-k_1 t} + A_2 e^{-k_2 t} + C \qquad (6)$$

where Y is the absorbance, A_1 and A_2 are the amplitudes of the absorbance changes of the first and second phase, respectively, k_1 and k_2 are the observed rate constants for each phase, and C is a constant to account for a non-zero baseline. The analysis of the data in Figure 3 yielded the following values: $k_1 = 20.2 \pm 0.6$ s^{-1} and $k_2 = 0.52 \pm 0.01$ s^{-1}. A calculated spectrum of the intermediate derived from this analysis is shown in Figure 3D. The rate constants that were obtained from the analyses of the data at different pH values are listed in Table 1.

Table 1: Dependence on pH of Rate Constants for the Oxidation of *N*-Semiquinone MADH by Amicyanin and Correlation with Steady-State Kinetic Parameters

pH[a]	k_1 (s^{-1})[b]	k_2 (s^{-1})[b]	k_{cat} (s^{-1})[c]
7.0	20.2 ± 0.6	0.52 ± 0.01	5.9 ± 0.5
7.5	32.6 ± 0.5	0.98 ± 0.14	nd[d]
8.0	46.0 ± 0.9	4.73 ± 0.17	14.4 ± 1.2
9.0	81.7 ± 2.2	10.7 ± 0.6	nd

[a] Reactions were performed in 10 mM BTP buffer at the indicated pH. [b] Rate constants were obtained from two-exponential fits of the oxidation of *N*-semiquinone by amicyanin (eq 4). The rate constant k_1 corresponds to the conversion of *N*-semiquinone to *N*-quinone (eq 7), and k_2 corresponds to the conversion of *N*-quinone to *O*-quinone (eq 8). [c] Values of k_{cat} are for the steady-state reaction of methylamine and amicyanin with MADH as described in Experimental Procedures. [d] Not determined.

Oxidation of O-Semiquinone MADH by Amicyanin Is Monophasic. The electron transfer from *O*-semiquinone MADH is much faster than that from the *N*-semiquinone (*5*), so if the same relatively slow reacting intermediate species observed in Figure 3 was formed during the reaction of the *O*-semiquinone, then it should accumulate to an even greater extent. Under reaction conditions where the intermediate species in the oxidation of *N*-semiquinone MADH was observed, no accumulation of an intermediate species was seen during the oxidation of *O*-semiquinone MADH by amicyanin (data not shown). This was true for both the *O*-semiquinone that was generated by stoichiometric titration with dithionite and the *O*-semiquinone that was generated by irradiation of *O*-quinol MADH with long-wavelength UV light. Thus, the intermediate seen in Figure 3 is *N*-semiquinone specific. This strongly suggests that it still possesses the substrate-bound nitrogen atom and provides a clue as to what may be the intermediate structure.

Identity of the Intermediate Species in the Conversion of N-Semiquinone to O-Quinone. The most reasonable explanation for the kinetic results described above is that the partial reaction in eq 4 proceeds by a sequential mechanism. The *N*-semiquinone is first oxidized to an *N*-quinone, and then hydrolysis by water yields the *O*-quinone and ammonia. Although the calculated spectrum of the intermediate species (Figure 3D) may not represent the exact spectrum of the putative *N*-quinone intermediate, it is very similar to that of the iminoquinone form of MADH that was generated in vitro (discussed below).

The hydrolysis of the *N*-quinone is a reversible reaction. It should, therefore, be possible to form the *N*-quinone from the *O*-quinone by addition of excess ammonia. Addition of ammonium salts to oxidized MADH has been shown to cause perturbations of its absorption spectrum (*16*−*18*). This causes a bleaching of the absorption spectrum of the *O*-quinone MADH from *P. denitrificans* (*16*). A titration of MADH from bacterium W3A1 with NH_4Cl and NH_3 was biphasic, and it was concluded that the first phase reflected binding of ammonia to TTQ which produces an iminoquinone (*17*). The absorption spectrum of that species was qualitatively similar to the spectrum of the intermediate depicted in Figure 3D in that it had features similar to those of the *O*-quinone but a somewhat lower absorption of the major peak and a slight increase in absorbance around 330 nm. A qualitatively similar result was also observed with MADH from *Thiobacillus versutus* (*18*). Another TTQ enzyme, aromatic amine dehydrogenase, showed a similar spectral perturbation on addition of ammonia that was also concluded to reflect binding of ammonia to TTQ which forms an iminoquinone (*19*). It is difficult to compare these results because the enzymes from the different sources have slightly different absorption maxima and the ammonia titrations were performed at different pH values, which can influence the spectral properties of MADH in the presence of monovalent cations (*17*). However, these results strongly support the conclusion that the intermediate species detected in Figure 3 is the *N*-quinone form of TTQ in MADH.

Role of the N-Quinone in the Steady-State Reaction Mechanism of MADH. The rate constants for the two-step conversion of *N*-semiquinone MADH to quinone were correlated with the steady-state kinetic parameters for the MADH-catalyzed oxidation of methylamine by amicyanin (Table 1). At both pH 7.0 and 8.0 in 10 mM BTP buffer, the rate for the second phase of the oxidation of *N*-semiquinone MADH by amicyanin is significantly slower than the steady-state value of k_{cat}. This indicates that the reaction step in eq 4 which is described by the smaller second rate constant does not occur in the steady state. An explanation for this is that the smaller rate constant describes the hydrolysis by water of the TTQ *N*-quinone which forms ammonia and *O*-quinone. In the steady state with excess substrate present, methylamine rather than water initiates a nucleophilic attack at C6 to release ammonia and form the next TTQ−substrate imine adduct. To test this hypothesis, the oxidation of *N*-semiquinone by excess amicyanin was monitored in the presence of methylamine by rapid-scanning stopped-flow spectroscopy.

When methylamine is present during the oxidation of *N*-semiquinone MADH by amicyanin, multiple turnovers of the enzyme will occur. After the first catalytic cycle, most of the total enzyme will be present as the enzyme form which exists prior to the rate-limiting step in the overall reaction. When methylamine is present during the oxidation of *N*-semiquinone MADH by amicyanin, no accumulation of the intermediate *N*-quinone is observed (Figure 4). Thus, hydrolysis of the *N*-quinone is not rate-limiting, and cannot be occurring in the presence of methylamine. To explain the results depicted in Figure 4, a modified reaction mechanism for MADH is presented in Figure 5.

Previous studies (*20*, *21*) have indicated that the rate-limiting step in the steady-state reaction of MADH is release of the aldehyde from the enzyme−product adduct (see Figure 5). Analysis of the data depicted in Figure 4 reveals a monophasic change from the spectrum of the *N*-semiquinone to that of an intermediate with a spectrum similar to that of reduced MADH. This is consistent with the accumulation of the enzyme−product complex (intermediate **III** in Figure 5) which is hydrolyzed in the rate-limiting step to yield the aldehyde product and *N*-quinol (**IV**). The limiting first-order rate constant for the reaction in Figure 4, which describes the formation of intermediate **III**, will reflect the slowest reaction step in the overall catalytic cycle leading to the formation of this intermediate. The rate constant for the formation of intermediate **III**, as calculated from the data depicted in Figure 4, is comparable to the k_1 values listed in Table 1 that describe the conversion of the *N*-semiquinone (**V**) to the *N*-quinone (**VI**). This is expected to be the slowest step on going from the *N*-semiquinone (**V**) to intermediate

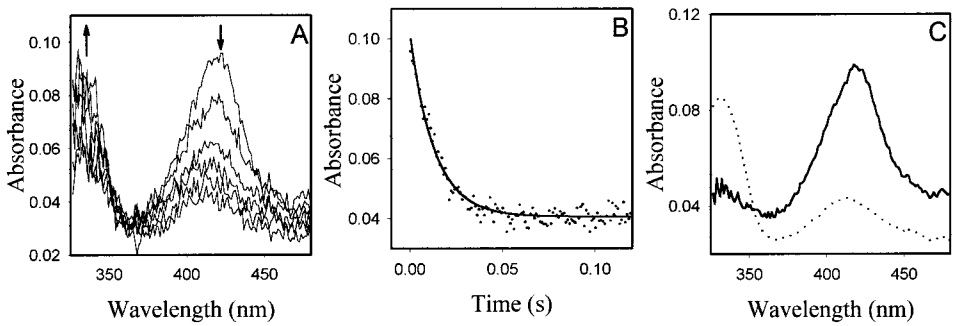

FIGURE 4: Reaction of *N*-semiquinone MADH with amicyanin in the presence of methylamine. The final reaction mixture contained 2 μM MADH, 20 μM amicyanin, and 100 μM methylamine in 10 mM BTP at pH 7.0 and 25 °C. (A) Spectra were recorded every millisecond. Those which are displayed were recorded after 1, 8, 17, 25, 29, 36, and 73 ms. Arrows indicate the directions of the spectral changes. (B) Analysis of the absorbance change with time at 420 nm. The solid line is a fit of the data to a single-exponential decay. (C) Calculated spectra. This plot displays a reconstruction of the initial (solid line) and final (dotted line) absorbing species for the A → B mechanism which best describes the data.

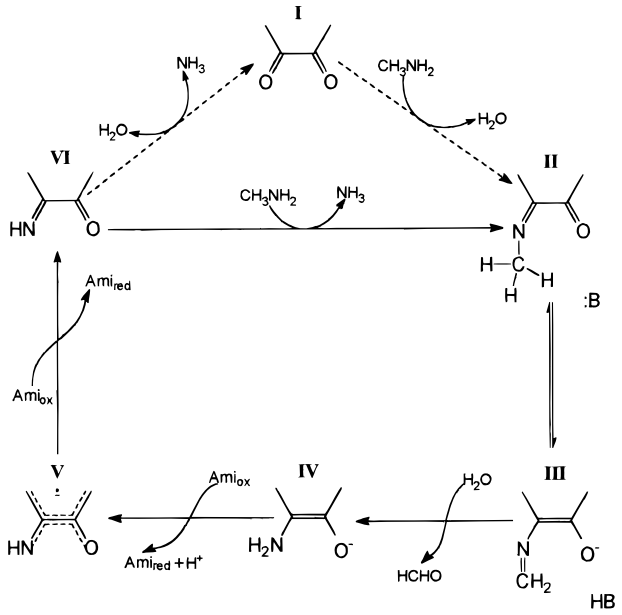

FIGURE 5: Proposed mechanism for the steady-state reaction of MADH with methylamine and amicyanin. Only the reactive portion of TTQ is shown. B represents an active site residue. The intermediate enzyme forms are labeled with Roman numerals so that they may be referred to in the text. Dashed lines indicate reactions that probably do not occur during the steady state in the presence of substrate. Ami_{ox} and Ami_{red} represent the oxidized and reduced forms of amicyanin, respectively.

III since the rate for the reduction of the enzyme−substrate complex (**II**) in forming the enzyme−product complex (**III**) is much faster (i.e., 275 s^{-1}) (*15*). On the basis of these results, it is clear that the oxidation of the *N*-semiquinone by amicyanin proceeds by a sequential mechanism, and eq 4 may be rewritten as two half-reactions (eqs 7 and 8).

$$N\text{-semiquinone} + \text{Ami}(Cu^{2+}) \rightarrow N\text{-quinone} + \text{Ami}(Cu^{+}) \quad (7)$$

$$N\text{-quinone} + H_2O \rightarrow O\text{-quinone} + NH_3 \quad (8)$$

These results also indicate that in the steady state, and in the physiological situation, the substrate reacts with the *N*-quinone (**VI**) intermediate form of MADH to form the next enzyme−substrate complex (**II**). Thus, the relevant reaction may be rewritten as eq 9.

$$CH_3NH_2 + N\text{-quinone} \rightarrow HCHO + N\text{-quinol} + NH_3 \quad (9)$$

The oxidized *O*-quinone form of TTQ (**I**) will only exist when there is no substrate present (i.e., the resting state).

pH and Salt Dependence of the Accumulation of the Intermediate. The oxidation of *N*-semiquinone MADH by amicyanin was studied in the absence of substrate over a range of pH in 10 mM BTP. The rate constants that were obtained for the biphasic reaction under saturating pseudo-first-order reaction conditions are listed in Table 1. The rate of the second phase of the reaction is much more dependent on pH than that of the first phase. Addition of salt to the buffer also causes a differential effect on the two rates. When 5 mM KCl was present in 10 mM BTP at pH 7.5, the first rate increased about 2.5-fold from 33 to 83 s^{-1}. In previous studies (*11*), it was also noted that the rate of this redox reaction exhibited a weak dependence on pH and salt concentration, similar to what was observed in this study. In contrast, the second rate increased about 10-fold from 0.97 to 9.4 s^{-1} upon addition of 5 mM KCl to the buffer. When the salt concentration was further increased, the reaction kinetics became monophasic because the rate of the second step becomes as fast or faster than that of the first phase (data not shown). Thus, it was not possible to fully examine the salt effect on the reactivity of the intermediate other than to say that the hydrolysis reaction (eq 8) is much more dependent on salt than the redox reaction (eq 7). It should be noted that previous studies on the mechanism of electron transfer from *N*-semiquinone MADH to amicyanin (*11*) were performed for the most part under experimental conditions where the *N*-quinone is hydrolyzed too fast for it to be a kinetically relevant and detectable intermediate. Therefore, conclusions from previous electron transfer studies are still valid and in no way compromised by the discovery that the conversion of the *N*-semiquinone to the *O*-quinone occurs by a two-step sequential mechanism.

The strong dependence on pH and salt of the rate of the hydrolysis of the *N*-quinone (eq 7) may be explained by the chemical mechanism by which imine hydrolysis reactions are known to occur. Imine hydrolysis reactions occur by addition of water to the C═N bond which forms a tetrahedral intermediate, followed by release of the amine, or in this case ammonia. At neutral and alkaline pH, the rate-limiting step for imine hydrolysis is the nucleophilic attack by water or hydroxide ion (*22*). The rate probably increases with pH

because a zwitterionic tetrahedral carbinolamine intermediate, with the amino N protonated and the hydoxyl O unprotonated, is necessary for release of ammonia. The concentration of this form of the tetrahedral intermediate will decrease as the pH decreases. The role of salt is less clear. MADH is known to bind monovalent cations at its active site, and this leads to spectral perturbations of oxidized MADH (*17*, *18*, *23*) and affects the reactivity of the *N*-quinol form of MADH (*9*). It is possible that a monovalent cation may also help to stabilize the zwitterionic carbinolamine by interacting with the unprotonated hydroxyl moiety, and account for the observed salt dependence.

Relevance to Other Enzymes with Different Carbonyl Cofactors. An important conclusion from this work is that with TTQ enzymes, the oxidized *O*-quinone form of the enzyme need not exist during the enzyme catalytic cycle. The nucleophilic amine substrate is capable of causing release of the ammonia product from the *N*-quinone intermediate that is concomitant with its forming the next enzyme−substrate adduct (Figure 5). Hydrolysis of the *N*-quinone by water is unnecessary. This is advantageous to the enzyme. It eliminates the need to design a specific feature of the active site to coordinate water and activate it for nucleophilic attack of the carbonyl C6. Instead, the site for substrate binding in the active site can serve this purpose as well. Direct nucleophilic attack of the imine also appears to be a more efficient reaction. The reaction mechanism in Figure 5 may be compared to that which is generally accepted for vitamin B_6-dependent enzymes (*24*). For these enzymes, the free carbonyl form of the pyridoxal phosphate (PLP) cofactor is not formed during the catalytic cycle, and the ϵ-amino group of a lysine residue forms a Schiff base with the cofactor when no substrate is present. The catalytic cycle is initiated by the reaction of the substrate amino group with the lysine−PLP internal aldimine which forms the substrate−PLP external aldimine. The significance of this feature to this discussion was demonstrated by site-directed mutagenesis studies of aspartate aminotransferase (*25*), in which conversion of this lysine to alanine caused a 10^4-fold decrease in the rate of external aldimine formation relative to that of the wild-type enzyme.

The catalytic cycle depicted in Figure 5 may also apply to enzymes that use other carbonyl cofactors that form Schiff base intermediates as both the initial enzyme−substrate adduct and the final enzyme−product adduct. Other cofactors which catalyze similar types of reactions include topaquinone (*26*), the cofactor of copper-containing amine oxidases, pyruvoyl cofactor (*27*) which is present in a variety of enzymes that decarboxylate amino acids and amino acid derivatives, and lysine tyrosylquinone (*28*) which is the cofactor of lysyl oxidase. As with TTQ, nucleophilic attack by an amine substrate of the enzyme−product Schiff base intermediate in the reaction cycle can allow release of the product that is concomitant with formation of the next enzyme−substrate Schiff base adduct. Hydrolysis by water to release product from the cofactor adduct need not occur, and the carbonyl forms of these cofactors (i.e., quinone, aldehyde, or ketone) probably do not exist in the presence of substrate.

REFERENCES

1. Davidson, V. L. (1993) in *Principles and Applications of Quinoproteins*, pp 73−95, Marcel Dekker, New York.
2. Husain, M., and Davidson, V. L. (1985) *J. Biol. Chem. 260*, 14626−14629.
3. Husain, M., and Davidson, V. L. (1985) *J. Biol. Chem. 261*, 8577−8580.
4. McIntire, W. S., Wemmer, D. E., Chistoserdov, A. Y., and Lidstrom, M. E. (1991) *Science 252*, 817−824.
5. Bishop, G. R., and Davidson, V. L. (1996) *Biochemistry 35*, 8948−8954.
6. Warncke, K., Brooks, H. B., Babcock, G. T., Davidson, V. L., and McCracken, J. L. (1993) *J. Am. Chem. Soc. 115*, 6464−6465.
7. Zhu, Z., and Davidson, V. L. (1998) *J. Biol. Chem. 273*, 14254−14260.
8. Bishop, G. R., and Davidson, V. L. (1995) *Biochemistry 34*, 12082−12086.
9. Bishop, G. R., and Davidson, V. L. (1997) *Biochemistry 36*, 13586−13592.
10. Davidson, V. L., Jones, L. H., and Kumar, M. A. (1990) *Biochemistry 29*, 10786−10791.
11. Bishop, G. R., and Davidson, V. L. (1998) *Biochemistry 37*, 11026−11032.
12. Zhu, Z., and Davidson, V. L. (1998) *Biochim. Biophys. Acta 1364*, 297−300.
13. Davidson V. L. (1990) *Methods Enzymol. 188*, 241−246.
14. Husain, M., Davidson, V. L., Gray, K. A., and Knaff, D. B. (1987) *Biochemistry 26*, 4139−4143.
15. Brooks, H. B., Jones, L. H., and Davidson, V. L. (1993) *Biochemistry 32*, 2725−2729.
16. Davidson, V. L., Brooks, H. B., Graichen, M. E., Jones, L. H., and Hyun, Y. (1995) *Methods Enzymol. 258*, 176−190.
17. Kuusk, V., and McIntire, W. S. (1994) *J. Biol. Chem. 269*, 26136−26143.
18. Gorren, A. C. F., and Duine, J. A. (1994) *Biochemistry 33*, 12202−12209.
19. Zhu, Z., and Davidson, V. L. (1998) *Biochem. J. 329*, 175−182.
20. Davidson, V. L., Jones, L. H., and Graichen, M. E. (1992) *Biochemistry 31*, 3385−3390.
21. Davidson, V. L., Graichen, M. E., and Jones, L. H. (1995) *Biochem. J. 308*, 487−492.
22. Cordes, E. H., and Jencks, W. P. (1963) *J. Am. Chem. Soc. 85*, 2843−2848.
23. Labesse, G., Ferrari, D., Chen, Z.-W., Rossi, G.-L., Kuusk, V., McIntire, W. S., and Mathews, F. S. (1998) *J. Biol. Chem. 273*, 25703−25712.
24. John, R. A. (1995) *Biochim. Biophys. Acta 1248*, 81−96.
25. Toney, M. D., and Kirsch, J. F. (1993) *Biochemistry 32*, 1471−1479.
26. Klinman, J. P., and Mu, D. (1994) *Annu. Rev. Biochem. 63*, 299−344.
27. Recsei, P. A., and Snell, E. S. (1984) *Annu. Rev. Biochem. 53*, 357−387.
28. Wang, S. X., Mure, M., Medzihradszky, K. F., Burlingame, A. L., Brown, D. E., Dooley, D. M., Smith, A. J., Kagan, H. M., and Klinman, J. P. (1996) *Science 273*, 1078−1083.

BI982939R